Effect of Quasihelical Symmetry on Trapped-Electron Mode Transport in the HSX Stellarator

W. Guttenfelder,[1,*] J. Lore,[1] D. T. Anderson,[1] F. S. B. Anderson,[1] J. M. Canik,[2] W. Dorland,[3] K. M. Likin,[1] and J. N. Talmadge[1]

[1]*Department of Electrical and Computer Engineering, University of Wisconsin–Madison, Madison, Wisconsin 53706, USA*
[2]*Oak Ridge National Laboratory, Oak Ridge, Tennessee 37831, USA*
[3]*Department of Physics, CSCAMM, IREAP, University of Maryland, College Park, Maryland 20742, USA*

(Received 18 July 2008; published 17 November 2008)

This Letter presents theory-based predictions of anomalous electron thermal transport in the Helically Symmetric eXperiment stellarator, using an axisymmetric trapped-electron mode drift wave model. The model relies on modifications to a tokamak geometry that approximate the quasihelical symmetry in the Helically Symmetric eXperiment (particle trapping and local curvature) and is supported by linear 3D gyrokinetic calculations. Transport simulations predict temperature profiles that agree with experimental profiles outside a normalized minor radius of $\rho > 0.3$ and energy confinement times that agree within 10% of measurements. The simulations can reproduce the large measured electron temperatures inside $\rho < 0.3$ if an approximation for turbulent transport suppression due to shear in the radial electric field is included.

DOI: 10.1103/PhysRevLett.101.215002 PACS numbers: 52.55.Hc, 52.25.Fi, 52.30.Gz

Stellarators are now routinely optimized to reduce neoclassical transport in the low collisionality regime [1]. The Helically Symmetric eXperiment (HSX) [2] was designed to have a magnetic field strength that is constant in a helical direction on a flux surface. It has been demonstrated experimentally that quasihelical symmetry (QHS) leads to reduced particle, momentum, and electron heat transport, consistent with predictions from neoclassical theory [3]. Because the neoclassical transport has been reduced to very small values, anomalous transport then dominates across the entire plasma. There is also experimental evidence in the Large Helical Device that the anomalous transport decreases for a magnetic configuration with improved neoclassical confinement [4]. The experimental observation that a quasisymmetric stellarator is dominated by anomalous transport, and the possible connection between reduced neoclassical and anomalous transport, motivates the theoretical and experimental understanding of turbulent transport in 3D geometries.

For 2D experiments, nonlinear, gyrokinetic turbulence simulations can provide first-principles, quantitative predictions of the transport in tokamaks [5]. However, such calculations are too expensive for routine use in transport simulations. Reduced models based on quasilinear transport expressions [6–9] have provided some success in predicting confinement [10]. These models are based on rapid linear stability calculations, coupled with mixing length estimates for the saturated fluctuation levels, implying that much (but not necessarily all) of the transport scaling is captured in the scaling of the linear instability.

Because of the lack of symmetry, increased complexity in geometry, and therefore increased computational expense, fewer linear and nonlinear simulations exist for stellarators. Recent linear gyrokinetic simulations in multiple stellarator configurations [11] demonstrate how differences in the magnetic field structure modify the linear growth rates from that of an axisymmetric geometry, for example, by changes in the overlapping regions of particle trapping and bad curvature. Additional differences are manifest in nonlinear simulations, where particle drift orbits in 3D geometry can alter the resulting turbulence saturation through their influence on zonal flows [12,13]. While the linear and nonlinear predictions in 3D geometry can differ quantitatively from a tokamak, the basic transport is theoretically expected to scale similarly with nondimensional parameters and to be similarly influenced by the thresholds and strengths of the linear microinstabilities. This is consistent with the similarity between tokamaks and stellarators of both the scaling of energy confinement [14] and the measured turbulence characteristics [15].

Since the magnetic field spectrum in HSX is dominated by a single helical component, for the most part there is a single class of trapped particles in the QHS configuration, just as in a tokamak. In this Letter, we present the first results of a model for the anomalous electron heat transport in HSX, making use of a tokamak quasilinear transport model for the trapped-electron mode (TEM) instability. It is demonstrated that replacing the trapped particle fraction and local curvature in a tokamak with values corresponding to the quasihelically symmetric field in HSX is crucial for properly modeling the temperature profile and confinement time.

The measured and modeled plasmas discussed in this Letter are produced and heated with $\leq$100 kW of injected power, using fundamental O-mode electron cyclotron resonance heating (ECRH) at 28 GHz with $B = 1.0$ T on the magnetic axis. With central heating, the electron temperature profiles are very peaked near the magnetic axis. An example of the profiles measured by Thomson scattering are shown in Fig. 1 for 100 kW of injected power, with $T_e(0) \approx 2.5$ keV. [The flux surface label $\rho = r/a = (\psi/\psi_{\mathrm{LCFS}})^{1/2}$ is used, where ψ (ψ_{LCFS}) is the toroidal

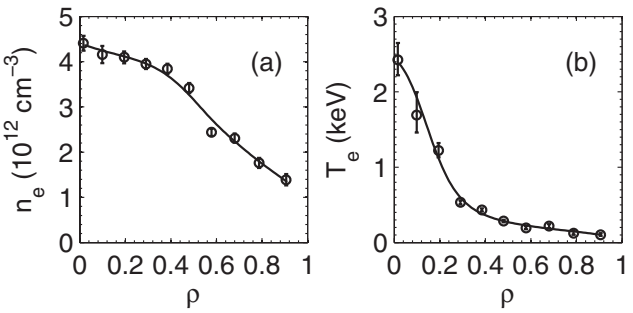

FIG. 1. Measured (a) electron density and (b) electron temperature profiles.

flux enclosed by a surface (last closed flux surface).] Measured impurity ion (C^{+5}, O^{+4}) temperatures are 40–80 eV.

Figure 2(a) shows the experimentally determined electron thermal diffusivity (χ_e) for the profiles in Fig. 1. Near the magnetic axis ($\rho \leq 0.2$), χ_e is as small as $\sim$0.6 m^2/s and increases to 5–10 m^2/s outside the midradius. These values can be compared to predictions of neoclassical transport, defined for particle and heat fluxes (for each species) by

$$\Gamma/n = -D_{11}\left(\frac{\nabla n}{n} - \frac{qE_r}{T}\right) - D_{12}\frac{\nabla T}{T}, \quad (1a)$$

$$Q/nT = -D_{21}\left(\frac{\nabla n}{n} - \frac{qE_r}{T}\right) - D_{22}\frac{\nabla T}{T}, \quad (1b)$$

where n is density, T is temperature, q is particle charge, and E_r is the radial electric field. The diffusion coefficients D_{ij} are determined by convolving the monoenergetic diffusion coefficients calculated by DKES [16] with a Maxwellian energy distribution. The electric field found via ambipolarity ($\Gamma_e = \Gamma_i$, assuming a pure hydrogen plasma) is shown in Fig. 2(b). Towards the plasma center, a large positive electric field is found, corresponding to the electron root. At the plasma edge, only the ion root with a small electric field is obtained. Near $\rho = 0.2$–0.3, more than one root exists. This transition region is modeled using a diffusion equation for the radial electric field [17]:

$$\frac{\partial E_r}{\partial t} - \frac{\partial}{\partial V}\left[\langle\nabla V\rangle D_E\left(\frac{\partial E_r}{\partial r} - \frac{E_r}{r}\right)\right] = \frac{e}{\varepsilon_\perp}(\Gamma_e - \Gamma_i), \quad (2)$$

where V is the volume enclosed by a flux surface, $\varepsilon_\perp = \varepsilon_0(1 + {V_A}^2/c^2)$, and V_A and c are the Alfvén and light velocities, respectively. The coefficient D_E approximates a diffusion coefficient for the radial electric field originating from perpendicular shear viscosity. Here we use a constant value (0.3 m^2/s) such that E_r reproduces values from calculations that conserve momentum and include parallel flows [18] (to be reported elsewhere). The corresponding neoclassical values of χ_e are shown in Fig. 2(a). Over the entire minor radius, the experimental χ_e is much larger than neoclassical, indicating a significant anomalous component.

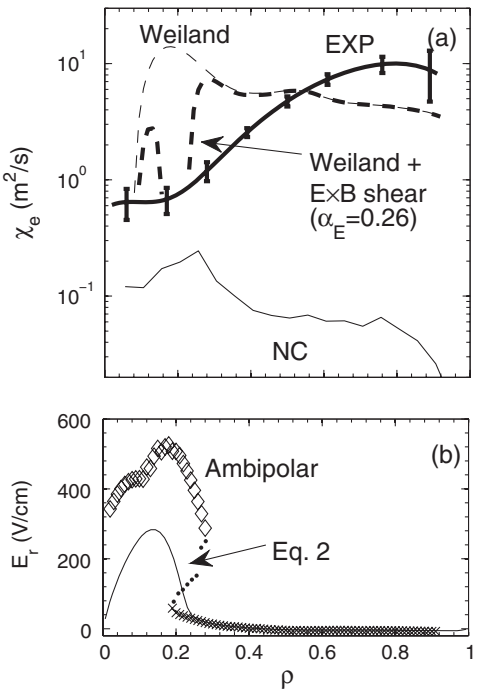

FIG. 2. (a) Electron thermal diffusivity from experiment, neoclassical theory, and the Weiland model. The thick dashed line includes the $E \times B$ quench rule with $\alpha_E = 0.26$. (b) Radial electric field determined from neoclassical theory using ambipolarity (electron root ◇, ion root ×, unstable root ●) or Eq. (2) (line).

For these plasmas, the helically trapped electrons are in the long mean-free-path regime across the minor radius. Given the low electron collisionality, the large ratio of T_e/T_i, and particle trapping due to the dominant helical ripple ε_H, the TEM is expected to be unstable. Following Ref. [19], the initial value, flux-tube gyrokinetic code GS2 [20] has been used to calculate linear growth rates of microinstabilities ($k_\perp \rho_s \sim 1$) in HSX. Magnetic equilibria are generated using VMEC [21], and the necessary geometry coefficients along a field line in the ballooning representation are calculated using TERPSICHORE [22] and VVBAL [23].

The calculations in this paper are performed on a field line domain centered at $\varphi = \theta = 0$, where minimum B and maximum local curvature (κ) and $\nabla B/B$ occur. The resulting eigenfunctions are strongly localized in this region. Figure 3(a) shows linear growth rates calculated for the $\rho = 0.86$ surface (using one kinetic ion species and kinetic electrons, $T_e/T_i = 2$, $a/L_{\mathrm{Ti}} = 0$, $\nu_e = \nu_i = 0$, maximized at $k_\theta \rho_s \approx 0.8$, with a ballooning parameter $\theta_0 = 0$). Normalized gradients are defined by $a/L_x = -1/x dx/d\rho$. The growth rates in Fig. 3(a) show that the instability is driven by gradients in both density and electron temperature, characteristic of the trapped-electron mode (real frequencies are in the electron diamagnetic drift direction). Scans over T_e/T_i, a/L_{Ti}, ν_e, and particle trapping $\sim {\varepsilon_H}^{1/2}$ (by varying minor radius) demonstrate

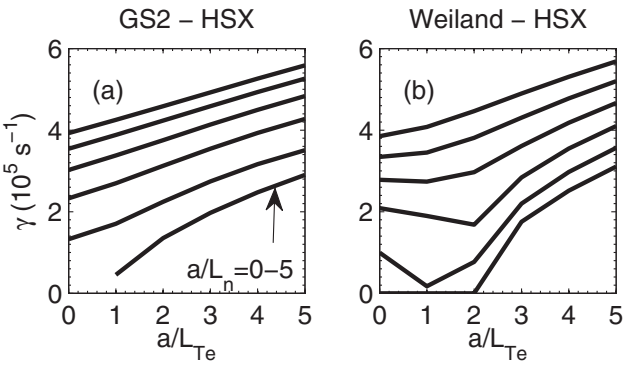

FIG. 3. (a) Growth rates calculated at different normalized density gradient (a/L_n) and electron temperature gradients (a/L_{Te}) using GS2 for HSX. (b) Growth rates calculated using the Weiland model with HSX approximations ($\varepsilon_T \rightarrow \varepsilon_H$, $R \rightarrow R/3$), as discussed in the text.

that the TEM instability in HSX scales similarly to that in tokamaks [24].

To model anomalous transport in HSX, the Weiland quasilinear transport model [6,7] for ion temperature gradient (ITG) and TEM instabilities is used. This model has been chosen as it provides linear growth rate predictions that can be compared with the GS2 calculations, as well as transport predictions for comparison to experiment. Only the main (hydrogen) ion species is included, and electron collisionality is set to zero. The Weiland model requires as input normalized gradients, the trapped particle fraction (f_t), and a single scale length (L_B) for the toroidal ($\nabla B/\kappa$) drifts. In a tokamak, the toroidal ripple $\varepsilon_T = r/R$ determines the trapped particle fraction $f_t = \sqrt{2\varepsilon_T/(1+\varepsilon_T)}$, and $L_B = R$. In HSX, the majority of trapped particles is determined by the dominant helical ripple in the quasisymmetric field $\varepsilon_H \approx 0.14r/a = 1.4r/R$. Because of small symmetry breaking terms, the actual trapped particle fraction is a little larger and does not go to zero on axis. Therefore, in the Weiland model f_t was adjusted to better match the growth rates at three radii where GS2 calculations were performed ($\rho = 0.24$, 0.51, and 0.86).

Because of the helical excursion of the magnetic axis, the curvature on the outboard side ($\varphi = \theta = 0$) is nearly 3 times larger than in a tokamak. Therefore, for modeling HSX, the toroidal scale length in the Weiland model is set to $L_B = R/3$. Figure 3(b) shows that the growth rates calculated using the Weiland model with HSX approximations reproduces the scaling *and* the magnitude of the GS2 growth rate calculations [Fig. 3(a)]. Without these approximations, the scaling with a/L_n and a/L_{Te} is weaker, leading to growth rates nearly 2 times smaller than the GS2 calculations. This illustrates directly the influence of the quasihelical geometry in HSX on the TEM instability.

Figure 2(a) shows that the value of χ_e calculated using the Weiland model is within ~2.5 times the experimental value outside $\rho > 0.4$, indicating that the trapped-electron mode is a plausible explanation for the anomalous transport in HSX. Around $\rho \sim 0.2$, where the measured electron temperature gradient is large (see Fig. 1), the predicted χ_e is 10–20 times larger than experimental. While the shape of χ_e predicted by the Weiland model does not recover the experimental profile shape within uncertainty, it is significantly better than a simple gyroBohm expression that would predict $\chi_e^{\mathrm{GB}} = (\rho_s/L_{\mathrm{Te}})T_e/B \sim 300\ \mathrm{m}^2/\mathrm{s}$ near the axis and ~3 m^2/s near the edge. This improved agreement depends specifically on the destabilizing influence of the trapped particle fraction and density gradient to the trapped-electron mode.

The above model prediction is very sensitive to the driving gradients, which are prone to large experimental uncertainty. An alternative test of the neoclassical and anomalous transport models can be made by predicting the T_e profile, given the input heating source rate profile (i.e., providing flux with small uncertainties). This is accomplished by numerically integrating the 1D flux-surface-averaged transport equation

$$\frac{3}{2} n_e \frac{\partial T_e}{\partial t} - \frac{\partial}{\partial V}[\langle \nabla V \rangle Q_e] = P_{\mathrm{ECRH}}(\rho),$$

where the transport (Q_e) is modeled as a sum of both neoclassical and Weiland contributions. The ECRH power deposition profile is calculated using a ray-tracing code, and the total absorbed power is determined from the time response of the diamagnetic flux loop during ECRH turnoff.

Figure 4(a) shows the resulting temperature profile predicted for the 100 kW plasma. For locations $\rho \geq 0.3$, the predicted T_e profile agrees within the 2σ uncertainty esti-

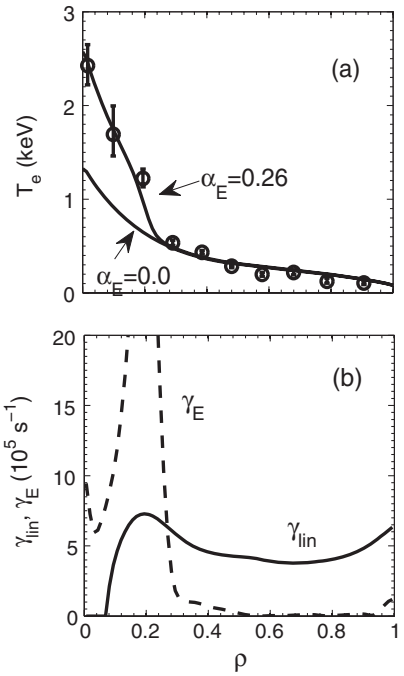

FIG. 4. (a) Predicted T_e profiles without ($\alpha_E = 0.0$) and with ($\alpha_E = 0.26$) $E \times B$ shear suppression. (b) Linear growth rate and $E \times B$ shear rate determined from experimental profiles.

mates for all experimental measurements (1σ shown in plots). The resulting electron energy confinement time (τ_E) agrees within 10% of the experimental value. Furthermore, for a range of injected powers down to 25 kW, there is comparable agreement between the experimental confinement times and the model. The predicted T_e profiles and energy confinement times using the Weiland model without the quasihelical geometry substitutions are 2–3 times larger than experimental, illustrating the significance of HSX geometry on TEM transport.

Inside $\rho < 0.3$, the large values of E_r minimize the neoclassical contribution, and it is the Weiland TEM transport that limits the simulated T_e to values smaller than the measurements. Calculations at $\rho = 0.24$ indicate that the growth rates from the Weiland model remain in reasonable agreement with GS2, suggesting that an additional mechanism may be important. The peaking of central temperature due to large radial electric fields is observed in many stellarator configurations [25] with strong on-axis heating (large P/n) and has been simulated previously using a generic gyroBohm transport model with $E \times B$ shear suppression [26]. Given the sharp transition in the E_r profile near $\rho \sim 0.2$ [Fig. 2(b)], a model for the suppression of turbulent transport via $E \times B$ shear is included through a ''quench rule'' [27] where the anomalous diffusivities are scaled by $\max[1 - \alpha_E \gamma_E/\gamma_{\max}, 0]$. $\gamma_E = (r/q)\partial(q v_{E\times B}/r)/\partial r$, and $\gamma_{\max}$ is the maximum linear growth rate in the absence of shear. Figure 4(b) is a plot of the shearing rate γ_E and $\gamma_{\max}$ as a function of radius. It can readily be seen that the region where the shearing rate is much greater than the growth rate corresponds very well to an increase in the electron temperature gradient, further justifying the shear suppression model.

In TEM-dominant axisymmetric nonlinear gyrokinetic simulations [27], $\gamma_E/\gamma_{\max} > 2.1$–$2.5$ is required for complete suppression of transport ($\alpha_E \approx 0.4$–0.5). In the transport simulations here, a value of $\alpha_E = 0.26$ is required to recover the peak electron temperature [shown in Fig. 4(a)], but this value depends on E_r [via D_E, Eq. (2)] as well as the linear growth rates from the TEM model. Increasing α_E further leads to a rapid increase of simulated $T_e(0)$. Nonlinear turbulence simulations demonstrating suppression of turbulent transport in stellarator geometry and a quantitative prediction of α_E will be required to provide a purely theory-based model of the core transport.

In summary, the Weiland ITG/TEM quasilinear transport model has been used to model plasmas in HSX. Using approximations for the dominant class of helically trapped particles and the increased value of local curvature, this model reproduces the scaling and magnitude of linear growth rates for the TEM instability in HSX as calculated by the 3D gyrokinetic code GS2. Using a predictive approach, simulated electron temperature profiles ($\rho \geq 0.3$) and energy confinement times agree with measured values. Simulations that include the quenching of turbulent transport indicate that $E \times B$ shear is important for predicting the peak temperature in HSX plasmas. These results demonstrate the impact of the local stellarator geometry on modeling anomalous transport, through changes in both microstability and $E \times B$ shear.

The authors thank W. A. Cooper for providing the TERPSICHORE and VVBAL codes, G. Rewoldt for providing FULL calculations for benchmarking, M. Barnes and D. Mikkelsen for assistance with the 3D GS2 calculations, and D. A. Spong for providing the PENTA code. This work was supported by the U.S. Department of Energy Contracts No. DE-FG02-93ER54222 and No. DE-FC02-04ER54784. Calculations were performed on the NERSC IBM SP3 supercomputer.

*Present address: Department of Physics, University of Warwick, CV4 7AL, United Kingdom.
w.guttenfelder@warwick.ac.uk

[1] H. E. Mynick, Phys. Plasmas **13**, 058102 (2006).
[2] F. S. B. Anderson *et al.*, Fusion Technol. **27**, 273 (1995).
[3] S. P. Gerhardt *et al.*, Phys. Rev. Lett. **94**, 015002 (2005); J. M. Canik *et al.*, Phys. Rev. Lett. **98**, 085002 (2007).
[4] H. Yamada *et al.*, Nucl. Fusion **41**, 901 (2001).
[5] J. Candy and R. E. Waltz, Phys. Rev. Lett. **91**, 045001 (2003).
[6] H. Nordman *et al.*, Nucl. Fusion **30**, 983 (1990).
[7] G. Bateman *et al.*, Phys. Plasmas **5**, 1793 (1998).
[8] M. Kotschenreuther *et al.*, Phys. Plasmas **2**, 2381 (1995).
[9] R. E. Waltz *et al.*, Phys. Plasmas **4**, 2482 (1997).
[10] ITER Physics Basis editors, Nucl. Fusion **39**, 2175 (1999).
[11] G. Rewoldt *et al.*, Phys. Plasmas **12**, 102512 (2005).
[12] P. Xanthopoulos *et al.*, Phys. Rev. Lett. **99**, 035002 (2007).
[13] T.-H. Watanabe *et al.*, Phys. Rev. Lett. **100**, 195002 (2008).
[14] U. Stroth *et al.*, Nucl. Fusion **36**, 1063 (1996).
[15] A. J. Wooton *et al.*, Plasma Phys. Controlled Fusion **34**, 2023 (1992).
[16] S. P. Hirshman *et al.*, Phys. Fluids **29**, 2951 (1986); W. I. van Rij and S. P. Hirshman, Phys. Fluids B **1**, 563 (1989).
[17] K. C. Shaing, Phys. Fluids **27**, 1567 (1984); H. Maassberg *et al.*, Phys. Fluids B **5**, 3627 (1993).
[18] D. A. Spong, Phys. Plasmas **12**, 056114 (2005).
[19] E. A. Belli *et al.*, Bull. Am. Phys. Soc. **46**, 232 (2001).
[20] M. Kotschenreuther *et al.*, Comput. Phys. Commun. **88**, 128 (1995).
[21] S. P. Hirshman and D. K. Lee, Comput. Phys. Commun. **39**, 161 (1986); S. P. Hirshman *et al.*, J. Comput. Phys. **87**, 396 (1990).
[22] D. V. Anderson *et al.*, Int. J. Supercomput. Appl. **4**, 34 (1990).
[23] W. A. Cooper, Plasma Phys. Controlled Fusion **34**, 1011 (1992).
[24] A. G. Peeters *et al.*, Phys. Plasmas **12**, 022505 (2005).
[25] M. Yokoyama *et al.*, Nucl. Fusion **47**, 1213 (2007).
[26] J. García *et al.*, Phys. Rev. Lett. **96**, 105007 (2006).
[27] J. E. Kinsey *et al.*, Phys. Plasmas **12**, 062302 (2005).